Effect of microstructure and slow crack growth on lifetime prediction of monolithic silicon carbide.

N. Al Nasiri[1], E. Saiz, F. Giuliani & L.J. Vandeperre

Centre for Advanced Structural Ceramics, Department of Materials, Imperial College London, South Kensington Campus, London SW7 2AZ, United Kingdom

Abstract

The lifetime of silicon carbide (SiC) based materials is strongly dependent on the presence of pre-existing flaws or cracks and their extension under an applied load during their service life. The purpose of this work is to determine the long term strength of SiC based materials with different grain morphologies and grain boundary chemistry. Solid state (SS) sintering of SiC with carbon and boron and liquid phase (LP) sintering of SiC using alumina and yttria as additives were used to produce fine and coarse grained materials to clarify the role of chemistry and grain morphology respectively. Fracture toughness, strength and slow crack growth (SCG) data were used to determine lifetime diagrams to accurately evaluate the long term strength behaviour for natural and artificial defects. The LP-SiC materials have more susceptibility to SCG compared to SS-SiC. However, the LP- SiC with coarse grains has a higher toughness and can be used at higher stresses after a large defect has been accidentally introduced. This indicates that the effect of the slow crack growth as a result of introducing oxides on the grain boundaries is not sufficient to alter the ranking between materials in terms of their deterministic allowable stress after such a damage event. On the other hand, the allowable stress in terms of the natural defect population revealed different results for using a low probability of failure (5%) and a much higher probability of failure (63.2%): the ranking of the materials alters when the stress level at which it is to be used changes.

Keywords: SiC, lifetime, strength, SCG and toughness.

[1] Corresponding author. Tel: +44 207 5895111
Email address: n.al-nasiri10@imperial.ac.uk

1. Introduction

Silicon carbide's properties such as a high specific stiffness, low thermal expansion and high thermal conductivity, make it an interesting structural material for space applications. Recent examples are the 3.5 m diameter silicon carbide primary mirror on ESA's Herschel telescope [1] and the large tubular ring on the ESA's GAIA mission [2]. Reducing the mass of space components ideally requires that the materials should carry as much load as possible and therefore using a high toughness silicon carbide appears promising. Moreover, due to the wear resistance and chemical inertness of ceramic materials, silicon carbide is becoming a potential candidate for biomedical applications such as orthopaedic implants [3, 4], where the components will be stressed for prolonged time in wet environments and here slow crack growth plays an important role in reducing strength and hence shortening the service lifetime of such components.

In addition to high toughness and sensitivity to slow crack growth, one should also consider strength reliability. It is known that the use of ceramic materials is limited in many applications due to the low strength reliability or the large variability in distribution of crack size and shape [5]. For identical specimens under identical loading conditions, the strength can vary unpredictably from sample to sample making it less reliable for engineering design [6]. Therefore, in order to understand the performance of silicon carbide materials and be able to design with them, one may consider the relationship between the variation in mechanical properties in terms of toughness and strength and the slow crack growth behaviour.

The aim of this paper is to evaluate the service life of the different types of silicon carbide as a function of the applied stress so that the relevance of all property measurements carried out can be highlighted. Since flaws can be introduced during production of the materials or by accidental damage after production, the material selection problem will be considered both for artificial flaws introduced by an incident as well as for the natural defects. In both cases the slow crack growth parameters in wet conditions will be used as a worst case scenario in terms of a reduction in the allowable stress for a desired service life.

2. Experimental methods

2.1 Material processing

For solid state sintering 3 wt.% carbon and different contents of boron (Grade II, H.C. Starck, Germany) were used [7]. Fine grains were achieved by hot pressing α-SiC (UF-25, H.C. Starck, Germany) at 2050 °C for 30 minutes with 0.2 wt.% boron. A bimodal microstructure with elongated grains was obtained by increasing the boron content to 0.5 w.t% and hot pressing β-SiC (BF-17, H.C. Starck, Germany) at 2150 °C for 3 hours. The carbon was added in the form of a phenolic resin (CR-96, Novolak, Crios Resinas, Brazil) with 50% carbon yield after pyrolysis at 400^0C for 1 hour in argon atmosphere.

For the liquid phase sintered materials, a mixture of 6 wt.% of aluminium oxide (AKP-30, Sumitomo, Japan) and 4 wt.% yttrium oxide (Grade C, H.C. Starck, Germany) was used as sintering additives. The fine equi-axed material was produced by hot pressing α-SiC at 1950 °C for 30 minutes, whereas the larger grain material was obtained by hot pressing β-SiC at 2050 °C for 3 hours [8-11].

The SiC powder and additives were mixed by ball milling for 24h using silicon nitride media (Union Process, Akron, USA) for the non-oxide mixture and alumina media for the oxide mixture (Union Process, Akron, USA) both in methyl ethyl ketone (VWR, London, UK). The slurries were dried by means of rotary evaporator R-20 (BUCHI Rotavapor, Switzerland). After drying, the powders were crushed and sieved through a 100 μm sieve. Hot pressing was conducted in an 80 mm graphite dies at heating rate of 10^0C min^{-1} under flowing argon gas in a graphite hot press (FCT, Rauenstein, Germany) under 25 MPa pressure.

2.2 Characterisation

The microstructure was examined using a scanning electron microscope (SEM, S-3400N, Hitachi, Japan). The specimens were polished to 1 μm using diamond suspension and chemically etched using boiling Murakami's solution [12]. The average grain size of 300 grains was calculated using the linear intercept method according to the approach of Mendelson [13].

The density was determined by Archimedes method with distilled water as the immersion medium according to ASTM standard C8300-00 [14]. The densities were compared to a theoretical density value of 3.28 g/cm^3 and 3.21 g/cm^3 for the SiC with oxide mixture and non-oxide mixture respectively.

Fracture toughness measurements in 3 point bending were performed according to ASTM 1421 using the single notched edge beam (SENB) method [15]. Specimens were 4 mm by 3 mm by 40 mm with root notch radius of 15 µm achieved by sharpening the notch using razor blade machine. A total number of five specimens for each material were tested in air at cross head speed of 0.05 mm min^{-1}. The average notch length was measured from both fracture surfaces.

The flexural strength was measured using 4 point bending according to ASTM C1161-02C. Specimens measuring 4 mm by 3 mm by 40 mm and their edges were bevelled to eliminate any stress concentration from machining. The tensile surfaces were polished to 1 µm using diamond suspension. A total number of 17 specimens were tested in air for each material at cross head speed of 1 mm min^{-1} and the average strength was calculated. The Weibull distribution [16]:

$$P_f = 1 - \exp\left[-\left(\frac{\sigma}{\sigma_0}\right)^m\right] \qquad \textbf{Equation 1}$$

was used to obtain the characteristic strength (σ_0) and Weibull modulus. In this expression, P_f is the probability of failure, which was estimated for each sample using [17]:

$$P_j = \frac{j - 0.3}{N + 0.4} \qquad \textbf{Equation 2}$$

where, j represents the rank number of a sample in terms of strength (j = 1 for the lowest strength sample) and N is the total number of tested samples.

Slow crack growth (SCG) testing was carried out using the constant stress rate test [18]. Specimens were 4 mm by 3 mm by 40 mm and edges were bevelled and polished to 1 µm using diamond

suspension. A 2 kg Vickers indent was placed in the centre of the tensile face with the orientation of the indent such that 2 of the cracks emanating from the corners created a crack perpendicular to the applied tensile stress. The indentations were made in air with 10 seconds holding time immediately prior to starting the bend test immersed in distilled water. The fracture stress was measured with an inner span of 10 mm and outer span of 20 mm at cross head speeds ranging from 0.001 mm min^{-1} to 1 mm min^{-1}. Additionally, inert strength values in oil were measured at crosshead speed of 1 mm min^{-1}. For every test, the fracture force and time were recorded in order to calculate the fracture stress and stress rate. A total of 5 specimens were tested at each stress rate for each material. To determine the slow crack growth parameter, the following was used [19]:

$$v = AK_I^n \qquad \textbf{Equation 3}$$

where, $\boldsymbol{v}$ is the crack velocity, K_I is the applied stress intensity factor, A and n are material and environment dependent subcritical crack growth parameters. The slope of log (failure stress) versus the log (stress rate), $\boldsymbol{n'}$, was converted using [20]:

$$n = \frac{4n' - 2}{3} \qquad \textbf{Equation 4}$$

The SCG parameter A was calculated using the following approach [21, 22]:

$$\sigma_f^{(n+1)} = \left[(n+1) \cdot \dot{\sigma} \cdot \sigma_{inert}^{(n-2)} \cdot \frac{2}{(n-2) \cdot A \cdot Y^2 \cdot K_{IC}^{(n-2)}} \right] \qquad \textbf{Equation 5}$$

where, σ_f is the fracture stress, $\dot{\sigma}$ is the applied stress rate, K_{IC} is the fracture toughness, σ_{inert} is the inert strength measured in oil and Y is a geometric constant depending on the type and shape of flaw. In this analysis, Y is taken as 1.12, which corresponds to small crack length [23].

The size of the pre-existing defect, a_i can be calculated from the inert strength, σ_{inert}, and toughness, K_{IC}, of the material after introduction of the damage:

$$a_i = \frac{1}{\pi} \cdot \left(\frac{K_{IC}}{Y \cdot \sigma_{inert}} \right)^2$$ **Equation 6**

During slow crack growth in wet environment, such pre-existing cracks will grow at stress level much lower than the critical value and fracture will occur once the crack length reaches a critical value at a given stress. Hence, the defect size where failure will occur can be calculated from:

$$a_f = \frac{1}{\pi} \cdot \left(\frac{K_{IC}}{Y \cdot \sigma_{service}} \right)^2$$ **Equation 7**

From fracture mechanics the following applies for a specimen under tensile loading (σ) with a certain crack length (a) [19]:

$$K_I = \sigma \cdot Y \cdot \sqrt{a\pi}$$ **Equation 8**

Substituting Equation 8 into Equation 3 and integrating with respect to crack length and time, the predicted lifetime, t_{life} can be obtained using the following [19]:

$$\frac{a_f^{-n/2+1} - a_i^{-n/2+1}}{1 - n/2} = A \cdot \sigma^n \cdot Y^n \cdot \pi^{n/2} \cdot t_{life}$$ **Equation 9**

where, a_f and a_i are the final and initial crack length and can be calculated using equation 6 and 7. The measured inert strength in oil from the constant stress rate test and the measured K_{IC} values from SENB test are used to obtain initial crack length, a_i and the variable service stress values are used to determine a_f. For each calculated final crack length and using the slow crack growth parameters A and n, the expected lifetime is obtained for the studied materials using equation Equation 9.

In order to determine the strength versus lifetime based on natural defects, two cases of time dependent strength are considered in this analysis. For case one, the initial strength value corresponds to 5% probability of failure (lower limit) and case two contains an initial strength of 63.2% probability of failure (upper limit). The lifetime under constant stress is calculated using the approach explained above using again the SCG data for water as a worst case scenario.

3. Results and Discussion

The microstructures of the four studied materials are shown in Figure 1. The LP-Fine SiC consists of homogenous fine equiaxed SiC grains with average grain size of 1.0 ± 0.1 µm. The large grains in the LP-Coarse SiC have an average length of 16 ± 1 µm and width of 5 ± 0.3 µm. For the SS-Fine SiC, the grains have an average grain size of 4.0 ± 0.4 µm and the large grains in the SS-Coarse SiC have an average length of 18 ± 1 µm and a width of 5 ± 0.3 µm. Table 1 shows a summary of all measured fracture mechanics parameters and SCG data.

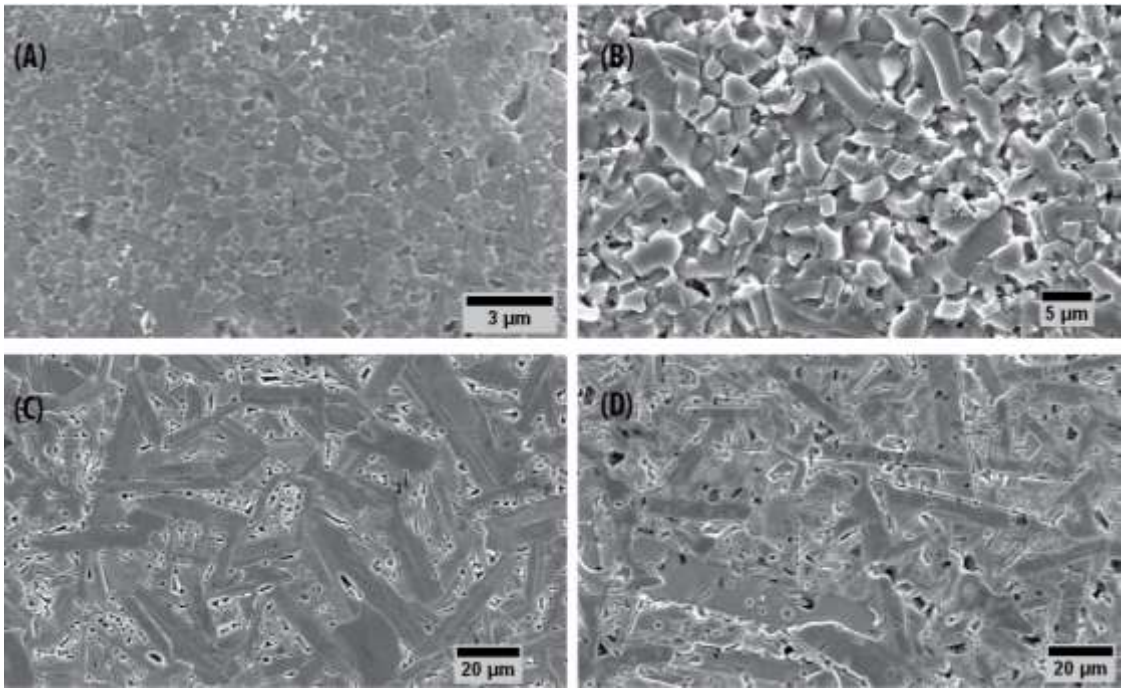


Figure 1: Scanning electron micrographs of chemically etched silicon carbide: (A) LP-Fine SiC, (B) SS-Fine SiC, (C) LP-Coarse SiC and (D) SS-Coarse SiC.

The fracture toughness (K_{IC}) values of the four SiC materials are shown in Table 1. The toughness (K_{IC}) is improved using liquid phase sintering and further increases are achieved by introducing elongated grains. This improvement is more noticeable in the liquid phase sintered materials than in the solid state sintered materials due to the fact that the SS-SiC materials have transgranular fracture mode, while it is intergranular fracture for the LP-SiC materials, which facilitate crack deflection and grain bridging [24, 25].

The fracture stress in water of the indented samples as a function of the stressing rate is plotted in Figure 2. The higher toughness of the liquid phase sintered SiC's, leads to higher fracture stress for indents produced with the same load, but more important is the fact that the fracture stress of the solid state sintered SiC's hardly varies with loading rate, whereas the fracture stress of the liquid phase sintered materials decreases when the loading rate is reduced.

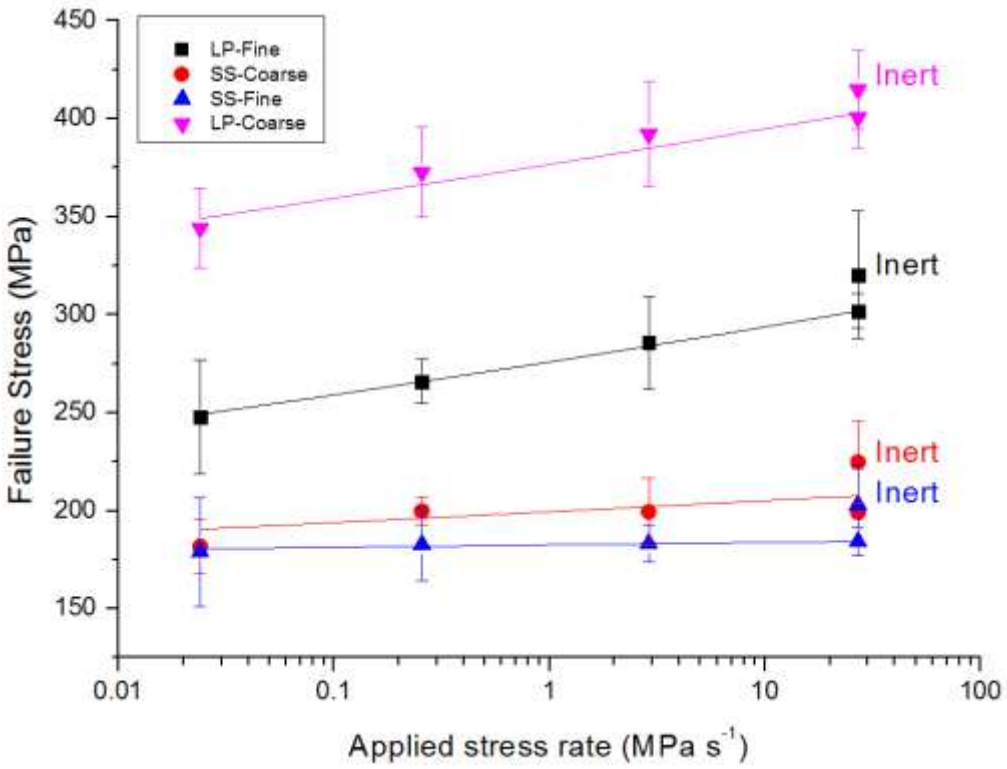


Figure 2: Failure stress versus stress rate of the four SiC materials in water with their corresponding inert strength measured in oil. The test was performed on indented SiC samples.

The exponents, *n*, and the values for the fracture stress measured in oil are listed in Table 1. The insensitivity to slow crack growth of the solid state SiC is reflected in the higher value of *n* comparing to the ones of the liquid phase sintered materials, which is consistent with observations elsewhere [26-29]. It is suggested that the oxide complexions along the grain boundaries make the LP-SiC materials prone to stress corrosion [30], because slow crack growth occurs as a result of a chemical reaction between water molecules and the metal–oxide (M-O bonds) [31]. It is also noticeable that the

materials with coarse grains exhibit higher *n* values in contrast to materials with fine grains, which is in agreement with work done on alumina and silicon nitride ceramics [29, 32, 33].

	LP-Fine	LP-Coarse	SS-Fine	SS-Coarse
Additives	6wt%Al_2O_3 4wt% Y_2O_3	6wt%Al_2O_3 4wt% Y_2O_3	3 wt% C 0.2 wt% B	3 wt% C 0.5 wt% B
Sintering conditions	1950 °C 0.5 h	2050 °C 3.0 h	2050 °C 0.5 h	2150 °C 3.0 h
Relative density, %	99.8 ± 0.1%	99.2 ± 0.1%	98.8 ± 0.2%	98.2 ±0.1%
Fracture toughness (K_{IC}), $MPam^{1/2}$	4.2 ± 0.3	6.5 ± 0.4	3.2 ± 0.4	3.7 ± 0.3
Data generated from indented SiC				
Inert strength in oil, (σ_{inert}), MPa	320 ± 32	415 ± 30	203 ± 20	222 ± 21
Slow crack growth exponent, *n*	41 ± 5	60 ± 11	108 ± 10	340 ± 18
Slow crack growth constant, *A*	1.19×10^{-22}	1.79×10^{-49}	2.49×10^{-52}	6.3×10^{-192}
Data generated from un-indented SiC				
Strength (σ), MPa	614 ± 79	441 ± 17	320 ± 127	375 ± 113
Characteristic strength (σ_0), MPa	650 ± 37	457 ± 17	362 ± 60	417 ± 55
Weibull modulus, (m)	8.3 ± 0.6	13.2 ± 0.5	2.8 ± 0.5	3.6 ± 0.6

Table 1: Summary of the measured fracture mechanics and SCG parameters for both indented and un-indented SiC.

The maximum allowable stress as a function of the desired lifetime is shown in Figure 3. The selected stresses are derived from calculations based on the toughness values and slow crack growth data. Figure 3 shows that LP-Coarse can be used in applications at much higher stresses and survives the same lifetime compared to the other three materials. This shows that the toughest silicon carbide (LP-Coarse) of this study even when taking into account its lower resistance to slow crack growth compared to the solid state materials, can be considered superior to the rest. LP-Fine clearly shows a very poor strength performance compared to the other three materials. This suggests that having coarse grains in the liquid phase sintered materials is advantageous for the long-term strength performance. However, this is not the case for the solid state sintered materials due to the similar strength performance for the same lifetime.

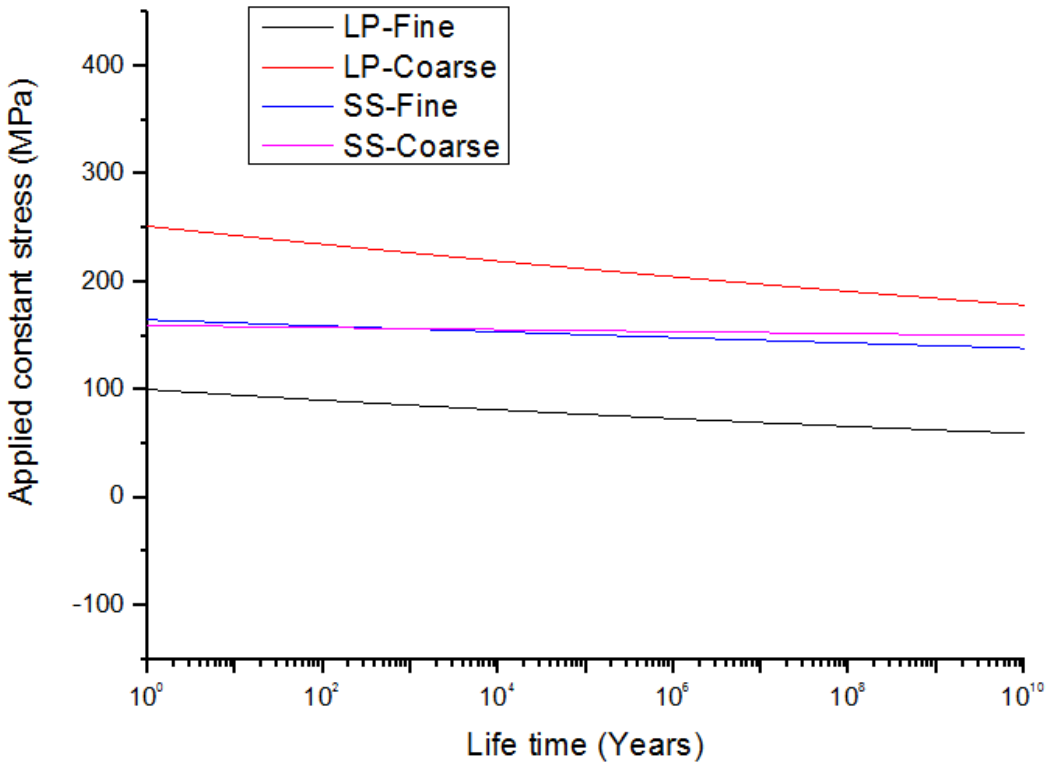


Figure 3: Maximum allowable stress as a function of the desired lifetime. The test was performed on indented SiC.

Figure 4 shows Weibull plots for the measured strengths from natural defects of each material based on 17 measurements. The Weibull parameters; Weibull modulus (m) and the characteristic strength (σ_0) are determined from the slope and intercept and are listed in Table 1. The Weibull modulus represents the scatter band of the strength distribution, where higher value gives less scatter and hence more reliability during design. The characteristic strength ($\sigma_{Pf=63.2}$) represents the strength at which 63.2% of the samples will have failed.

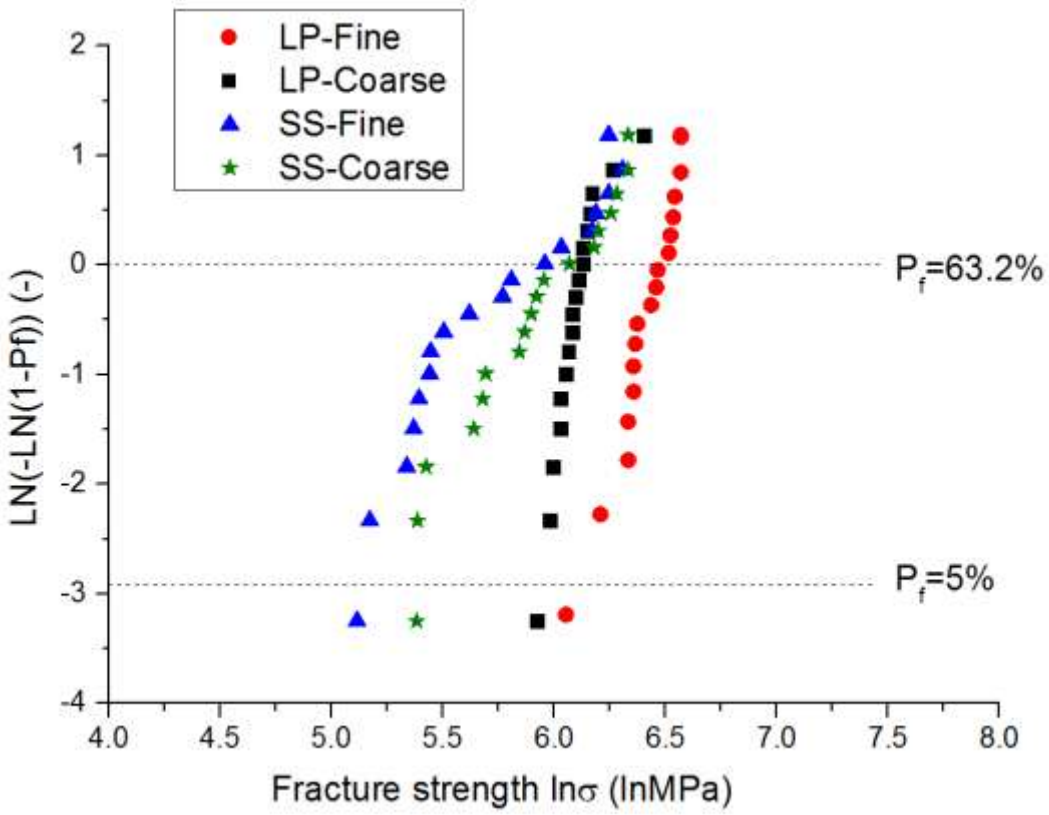


Figure 4: Weibull distribution diagram obtained for the un-indented SiC samples. Dashed lines showing the probability of failure equals 5 and 63.2%.

The obtained *m* values are in line with typical values ranging from 3 to 12 for ceramic materials [34]. Care was taken to ensure all specimens had the same surface finish prior to testing so that the values obtained here must be related to real differences between the materials. The very low *m* values obtained for the SS-SiC indicate that the defect sizes are non-uniformly distributed within the material. On the other hand, the LP-SiC specimens show a higher Weibull modulus suggesting a more uniform distribution of flaws with less strength variation between different specimens of the same material. For the solid state sintered materials, the flaw size did not depend on grain size and therefore finds its origin in other processing defects such as carbon inclusions, which by their nature are more variable.

From Figure 5, it can be seen that at the lower end of the probability of failure scale (5%), the LP-Coarse again shows a superior strength even for a long service life compared to the rest. Lifetime

predictions of LP-Coarse after 1 day and 10 years indicate an allowable stress reduction of 6% and 13% respectively. On the other hand, LP-Fine shows a dramatic allowable stress deterioration of 20% and 25% after 1 day and 10 years respectively. Moreover, if a survival time of 1 year is required, the applied stress cannot exceed 156 MPa compared to 256 MPa for LP-Coarse. SS-Fine has a moderate allowable stress degradation of 14% if 10 years of service is needed, while the allowable stress of SS-Coarse decreases by 6% only after 10 years. This result suggest that coarse grained material and hence higher toughness show better strength performance for 10 years of service compared to the fine grained materials.

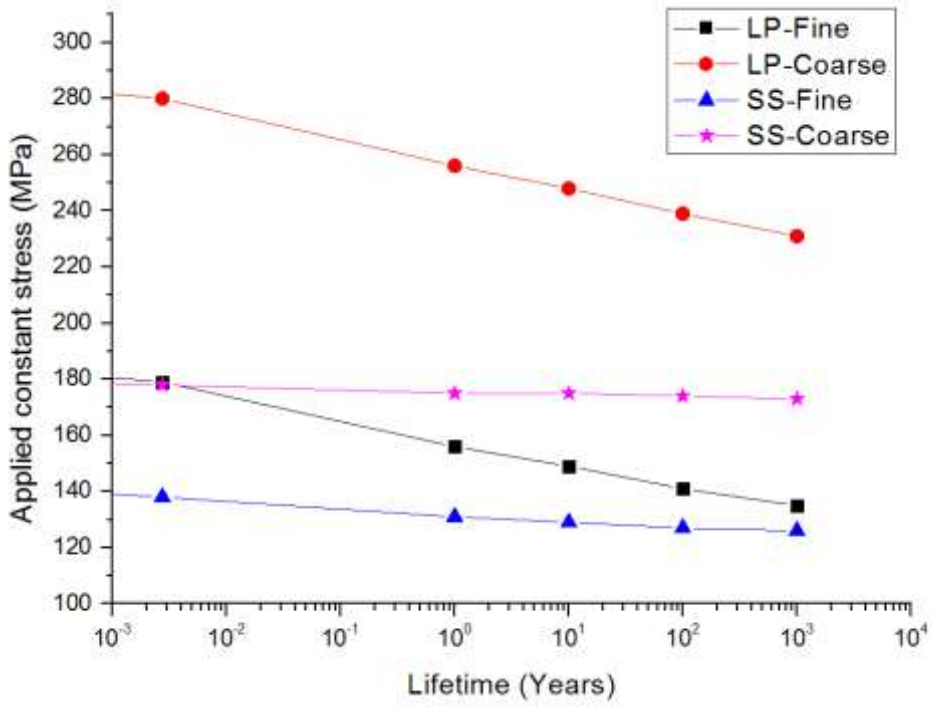


Figure 5: Maximum allowable stress versus lifetime for the un-indented SiC samples. The data is obtained from initial strength value at P_f = 5%.

For case two, where initial strength at higher probability of failure (63.2%) is used, SS-Coarse shows better performance after 1 and 10 years than LP-Coarse, Figure 6. The SS-Coarse shows a decrease in allowable stress of only 5% after 10 years compared to 17% of allowable stress degradation in LP-Coarse. Both LP-Fine and SS-Fine show strong reductions in allowable stress of 25% and 14% respectively after 10 years of service time in addition to the very low applied stresses. This change in the ranking as the acceptable probability in failure is altered, is not surprising when the Weibull plots

in Figure 44 are considered: the gap in allowable stress between the different materials decreases strongly as the stresses become higher and at the higher end of failure probabilities the inert strengths become equal. Since the solid state sintered materials suffer less environmental cracking, they will outperform the liquid phase sintered materials in the high stress regime.

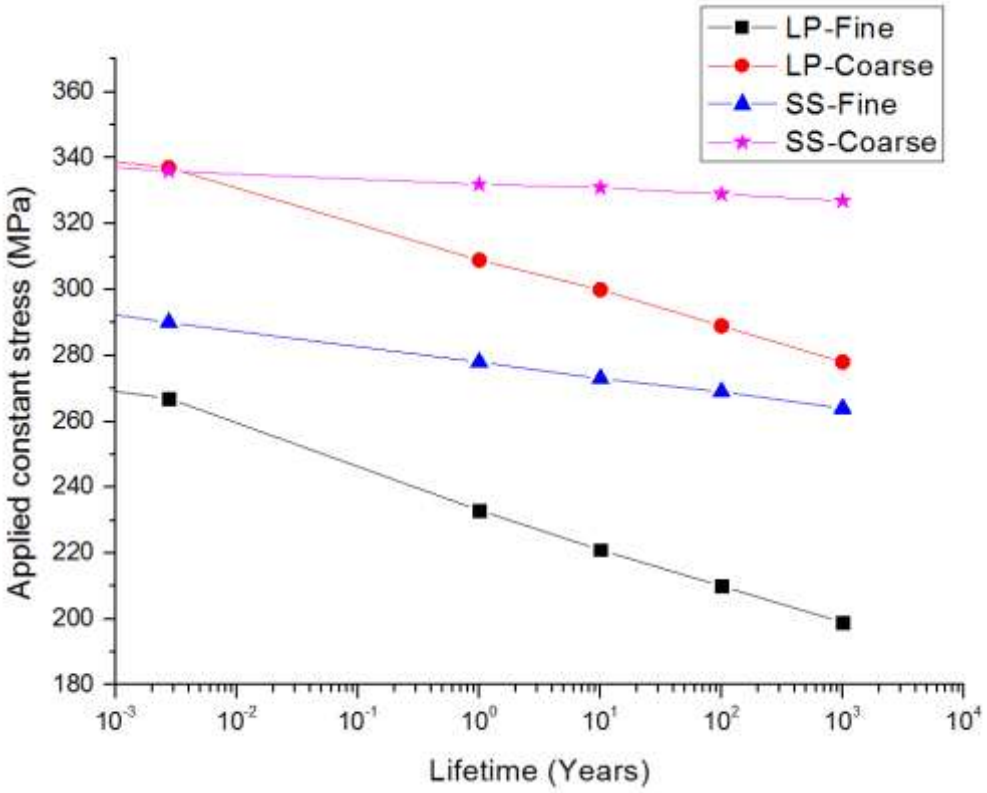


Figure 6: Maximum allowable stress versus lifetime for the un-indented SiC samples. The data is obtained from initial strength value at P_f = 63.2%.

The SS-Coarse shows a better performance for stresses used at higher probability of failure (63.2%) compared to those at 5% probability of failure, see Figure 6. In general maximising the stresses in a component enhances the material efficiency and hence allows reducing the mass of components. Hence high applied stresses are highly desirable. Whether a 63.2% probability of failure, i.e. more than 1 in 2 components will fail, is problematic depends on whether the risk can be mitigated appropriately and the value gained in using such high stresses. If the value of a component is too low to warrant producing roughly double the number required, then obviously lower stresses must be

selected, whereas if an ambitious project becomes possible only if high stresses are used, the cost of manufacturing spare components could easily be negligible compared to the total cost of the project.

From the above, one may conclude that at lower fracture probability, i.e. for relatively inexpensive components, the LP-Coarse is superior as its high toughness leads to less variability in strength and the slow crack growth in such situations does not really affect the time of survival performance in wet conditions. However, if using the material near the highest stresses is an essential condition, it seems that the SS-Coarse looks an appealing candidate to be considered.

4. Conclusions

It was shown that the larger damage tolerance of materials with a higher toughness enhances their ability to continue to perform at higher stresses after a large defect has been accidentally introduced. The effect of the slow crack growth as a result of introducing oxides on the grain boundaries is not sufficient to alter the ranking between materials in terms of their deterministic allowable stress after such a damage event and therefore if such damage is likely to occur, the liquid phase sintered SiC with coarse grains is without doubt the best material to use, followed by either of the solid state sintered SiC's and finally the liquid phase sintered fine grained material.

In a second case, the allowable stress in terms of the natural defect population was considered as a function of the service life. By considering both the case for a low probability of failure (5%) as well as one in which a much higher probability of failure is tolerated (63.2%), it was shown that the ranking of the materials alters when the stress level at which it is to be used changes. This is a consequence of the difference in strength determining defect distributions for solid state sintered materials and liquid phase sintered materials. In the latter, the strength determining defects are related to the grain size and since great effort was spent in creating well defined grain size distributions, the variation in strength is limited. In contrast, in solid state sintered materials the strength determining defects are more random, such as carbon inclusions and hence their Weibull modulus is markedly lower because such defects are inherently more variable. In this situation, material selection largely depends on the acceptable probability of failure of a component.

Acknowledgments

The authors would like to thank the Engineering and Physical Sciences Research Council (EPSRC) of the UK for the funding of this project through grant EP/F033605/1.

References

1. Agency, ESA. *Small French firm behind Herschel's giant mirror*. 2010; Available from: http://www.esa.int/SPECIALS/Technology/SEMBD6ZNZBG_0.html.
2. Agency, ESA; Available from: http:?//sci.esa.int/gaia/40129-payload-module/.
3. J. Will, A. Hoppe, F. Müller, C. Raya, J. Fernández, and P. Greil, *Bioactivation of biomorphous silicon carbide bone implants.* Acta Biomaterialia, 2010. **6**(12): p. 4488-4494.
4. J. Chevalier and L. Gremillard, *Ceramics for medical applications: A picture for the next 20 years.* Journal of the European Ceramic Society, 2009. **29**(7): p. 1245-1255.
5. M. Borba, M. de Araujo, K. Fukshima, H. Yoshimura, P. Cesar, J. Griggs, and A. Bona, *Effect of the microstructure on the lifetime of dental ceramics.* Dental Material Sceince, 2011. **27**(7): p. 710-721.
6. P. Warren, *Fracture of brittle materials: Effects of test method and threshold stress on the Weibull modulus.* Journal of the European Ceramic Society, 2001. **21**(3): p. 335-342.
7. L. Stobierski and A. Gubernat, *Sintering of silicon carbide II Effect of boron.* Ceramics international, 2003. **29**: p. 355-361.
8. N. Padture, *In situ toughened silicon carbide.* Journal of the American Ceramic Society, 1994. **77**(2): p. 519-523.

9. S. Lee and C. Kim, *Effects of alpha SiC versus beta SiC powders on microstructure and fracture toughness of SiC sintered with Al2O3-Y2O3 additives.* Journal of the American Ceramic Society, 1994. **77**(6): p. 1655-1658.

10. S.K. Lee, D.K. Kim, and C.H. Kim, *Flaw-tolerance and R-curve behavior of liquid phase sintered silicon carbide with different microstructures.* Journal of the American Ceramic Society, 1995. **78**(11): p. 65-70.

11. S.K. Lee, Y.C. Kim, and C.H. Kim, *Microstructural development and mechanical properties -sintered SiC with plate-like grains using Al2O3-Y2O3 additives.* Journal Materials Science, 1994. **29**: p. 5321-5326.

12. W. Lee and W. Rainforth, *Ceramic Microstructure*. 1994: Kluwer Academic Publishers.

13. M. Mendelson, *Average grain size in polycrystalline ceramics.* American Society for Testing and Materials, 1969. **52**(8): p. 443-446.

14. *ASTM C830-00: Standard Test Methods for Apparent Porosity, Liquid Absorption, Apparent Specific Gravity, and Bulk Density of Refractory Shapes byVacuum Pressure.* 2011: p. 1-5.

15. *ASTM C1421-10: Standard Test Methods for Determination of Fracture Toughness of Advanced Ceramics at Ambient Temperature.* The American Ceramic Society, 2010: p. 1-31.

16. W. Weibull, *A statistical distribution function of wide applicability.* Journal of applied Mechanics, 1951. **51**(A6): p. 293-296.

17. B. Bergman, *On the estimation of the Weibull modulus.* Journal of Materials Science Letters, 1984. **3**(8): p. 689-692.

18. S. M. Wiederhorn, *Subcritical crack growth in ceramics*, in *Fracture Mechanics in ceramics*, R.C. Bradt, D.P.H. Hasselman, and F.F. Lange, Editors. 1974, Pelnum Press: New York. p. 613-646.

19. B. Lawn, *Fracture of brittle solids*. 2n ed. 1993, Cambridge: Cambridge University Press.

20. E. Fuller, B. Lawn, and R. Cook, *Theory of fatigue for brittle flaws originating from residual stress concentrations.* Journal of The American Ceramic Society, 1983. **66**(5): p. 314-321.

21. F. Sudreau, C. Olagnon, and G. Fantozzi, *Lifetime prediction of ceramics: Importance of the test method.* Ceramics international, 1994. **20**(2): p. 125-135.

22. D. Kalish and B. Tariyal, *Static and Dynamic fatigue of a polymer-coated fused silica optical fiber.* The American Ceramic Society, 1977. **45**(G-77): p. 518-523.

23. U. Lohbauer, A. Petschelt, and P. Greil, *Lifetime prediction of CAD/CAM dental ceramics.* Journal of the American Ceramic Society, 2002. **63**(6): p. 780-785.

24. S. Lee, Y. Kim, and C. Kim, *Microstructural development and mechanical properties - sintered SiC with plate-like grains using Al2O3-Y2O3 additives.* Journal of Materials Science, 1994. **29**(20): p. 5321-5326.

25. K. Faber and A. Evans, *Intergranular crack-deflection toughening in silicon carbide.* Journal of the American Ceramic Society, 1983. **66**(6): p. C-94 - C-95.

26. R. Pabst and G. Popp, *Critical and subcritical crack extension in Al2O3 and SiC as functions of temperature, environment and loading rate*. Surface Flaws, Statistics and Microcracking, ed. R.C. Bradt, A.G. Evans, D.P.H. Hasselman, and F.F. Lange. Vol. 5. 1983, New York: Plenum Press.

27. Y. Yamauchi, S. Sakai, M. Ito, T. Ohji, W. Kanematsu, and S. Ito, *Dynamic fatigue behavior of ceramics at room temperature.* The Ceramic Society of Japan, 1988. **96**(9): p. 885-889.

28. G. Choi and S. Horibe, *Static fatigue in ceramic materials: Inflences of an intergranular glassy phase and fracture toughness.* Journal of Materials Science, 1993. **28**(21): p. 5931-5936.

29. S. Choi, J. Salem, and N. Nemeth, *High temperature slow crack growth of silicon carbide determined by constant stress rate and constant stress testing.* Journal of Materials Science, 1998. **33**(5): p. 1325-1332.

30. Al Nasiri, N., *Effect of grain boundary chemistry and grain morphology on the mechanical behaviour of silicon carbide*. Ph.D. 2014, Imperial College London: UK. p. 213.

31. S. Wiederhorn, *Subcritical crack growth in ceramics*, in *Fracture Mechanics in Ceramics*, R.C. Bradt, D.P.H. Hasselman, and F.F. Lange, Editors. 1974, Pelnum Press: New York. p. 613-646.

32. G. Himsolt, H. Knoch, H. Huebner, and F. Kleinlein, *Mechanical properties of hot pressed silicon nitride with different grain structures.* Journal of the American Ceramic Society, 1978. **62**(1-2): p. 29-32.

33. B. Pletka and S. Wiederhorn, *A comparison of failure predictions by strength and fracture mechanics techniques.* Journal of Materials Science, 1982. **17**(5): p. 1247-1268.

34. B. Basu, D. Tiwari, D. Kundu, and R. Prasad, *Is Weibul distribution the most approperiate statistical strength distribution for brittle materials?* Ceramic International, 2009. **35**(1): p. 537-546.